JACC Vol. 32, No. 4
October 1998:1096–101

Evaluation of Dynamic Changes in Microvascular Flow During Ischemia-Reperfusion by Myocardial Contrast Echocardiography

LEONARDA GALIUTO, MD,* ANTHONY N. DEMARIA, MD, FACC,*
KAREN MAY-NEWMAN, PHD,† UGHETTA DEL BALZO, PHD,† KOJI OHMORI, MD,*
VALMIK BHARGAVA, PHD, FACC,* STEPHEN F. FLAIM, PHD, FACC,†
SABINO ILICETO, MD, FACC‡

San Diego, California and Cagliari, Italy

Background. **Dynamic changes of myocardial blood flow have been observed after reperfusion of an occluded coronary artery. MCE performed by intracoronary contrast injection can provide an estimate of microvascular flow. We hypothesized that MCE performed using intravenous infusion of a new generation contrast agent and electrocardiogram-gated harmonic imaging would be able to assess serial changes of microvascular perfusion.**

Objective. **To study the potential of myocardial contrast echocardiography (MCE) to assess serial changes of microvascular flow during ischemia-reperfusion.**

Methods. **Sixteen dogs underwent 90 or 180 min of left anterior descending coronary occlusion, followed by 180 min of reperfusion. Regional blood flow (RBF) was measured with fluorescent microspheres at baseline, during coronary occlusion, and at 5, 30, 90, and 180 min during reperfusion. At the same time points, MCE was performed with intravenous infusion of AF0150 (4 mg/min). Gated end-systolic images in short axis were acquired in harmonic mode and digitized on-line. Background-subtracted videointensity measured from MCE and RBF obtained from fluorescent microspheres were calculated for the risk area and for a control area, and were expressed as the ratio of the two areas.**

Results. **After initial hyperemia, a progressive reduction in flow was observed during reperfusion. MCE correctly detected the time course of changes in flow during occlusion-reperfusion. Videointensity ratio significantly correlated with RBF data ($r = 0.79$; $p < 0.0001$).**

Conclusions. **The progressive reduction in blood flow occurring within the postischemic microcirculation was accurately detected by MCE. This approach has potential application in the evaluation and management of postischemic reperfusion in humans.**

(J Am Coll Cardiol 1998;32:1096–101)

The prompt reopening of the infarct-related artery is the major goal of the therapy of acute myocardial infarction. However, after prolonged myocardial ischemia, the microvascular network can be functionally and/or structurally damaged, and reopening an epicardial vessel may not be followed by adequate myocardial reperfusion, a condition referred to as "no- or low-reflow" phenomenon (1–4). The microvascular damage may be aggravated by reperfusion itself, a condition referred to as reperfusion injury (5–7). As a result of the evolving functional and structural microvascular damage, dynamic changes in the degree of reflow may occur within the postischemic microcirculation (6–10).

From the *Division of Cardiovascular Medicine, University of California, San Diego, California; †Alliance Pharmaceutical Corp., San Diego, California; and the ‡Institute of Cardiology, University of Cagliari, Cagliari, Italy. Dr. L. Galiuto is recipient of a grant from Consiglio Nazionale delle Richerche (CNR), Italy. The study was sponsored by Alliance Pharmaceutical Corp., San Diego, CA.

Presented in part at the 47th Annual Scientific Session of the American College of Cardiology, Atlanta, March 1998.

Manuscript received March 12, 1998; revised manuscript received June 2, 1998, accepted June 17, 1998.

Address for correspondence: Anthony N. DeMaria, MD, Division of Cardiovascular Medicine, University of California at San Diego, 200 West Arbor Drive, San Diego, California, 92103-8411. E-mail: ademaria@ucsd.edu.

In the setting of reperfused myocardial infarction, the extent of microvascular perfusion has been shown to predict the ultimate amount of myocardial damage and the extent of residual viability (11–15). Also, therapeutic interventions may be developed that have the potential to control or limit deleterious changes observed after postischemic reflow (16). Therefore, it would be important to have a method to detect and quantify myocardial microvascular flow and to follow it over time.

Myocardial contrast echocardiography (MCE) has many advantages as a technique to study the coronary microvasculature in vivo (17). Recently, several microbubbles have been created that, after venous injection, are able to transit the pulmonary circulation in sufficient number to opacify both the left ventricular (LV) cavity and the myocardial capillary bed (18,19). Therefore, the present study was designed to define the ability of MCE to assess microcirculatory perfusion during reflow after acute coronary occlusion.

Methods

Animal preparation. Sixteen open-chest mongrel dogs were subjected to either 90 or 180 min of coronary occlusion to produce infarct size of variable extent. Reperfusion was

0735-1097/98/$19.00
PII S0735-1097(98)00349-0

Abbreviations and Acronyms

LAD = left anterior descending artery
LCx = left circumflex artery
LV = left ventricular
MCE = myocardial contrast echocardiography
RBF = regional blood flow

achieved in all animals and maintained for 180 min. The animal studies were performed in accordance with the "Position of the American Heart Association on Research Animal Use."

The dogs were anesthetized (0.1–2.5 mg/kg of Propofol 1%; Zeneca Pharm.), intubated, and ventilated with a respiratory pump (model 55-0715; Harvard Apparatus). Additional anesthetic was administered as required. Body temperature was kept within physiologic limits by adjusting a heating blanket. The ECG was monitored continuously. Three 7F catheters were placed: left femoral artery for withdrawal of reference samples for blood flow measurements, right femoral artery to record arterial pressure, and left femoral vein to infuse drugs and fluids. A catheter (Swan-Ganz) monitored pulmonary artery pressures and measured cardiac output. A high-fidelity micromanometer-tipped LV catheter transducer recorded LV pressure. A lateral thoracotomy was performed and the heart was suspended in a pericardial cradle. A 7F silastic catheter was placed in the left atrium for injection of fluorescent microspheres. The proximal-mid part of the left anterior descending (LAD) was dissected free from surrounding tissue and an occluder was placed around it. An ultrasonic transit-time flow probe (2.0–2.5 mm) was placed proximal to the occluder and was connected to a flow meter (model T108; Transonic System Inc.) for digital measurement of flow.

Myocardial contrast echocardiography. Echocardiography was performed with a phased-array broad band 3–2–MHz transducer (HDI3000; ATL). Images were obtained by placing the transducer on a standoff consisting of a saline-filled latex bag positioned on the epicardium of the LV anterior wall. The transducer was maneuvered to yield a short axis view at the midpapillary muscle level and was subsequently fixed in place by a mechanical arm. The tomographic plane encompassing the LAD perfusion territory distal to the occluder was identified by the appearance of wall motion abnormalities produced by temporary coronary occlusion. Instrument settings were optimized during contrast administration, and were subsequently held constant. Echocardiographic imaging was performed using harmonic technology with ultrasound transmitted at 1.67 and received at 3.33 MHz. A dynamic range of 60 dB and a mechanical index of 0.9 were used, and ECG-triggered images were obtained at end-systole every six heart beats.

AF0150 (Imagent US; Alliance Pharmaceutical Corp), a perfluorochemical-stabilized contrast agent, was infused intravenously. A 100-mg vial of AF0150 was reconstituted with 10 mL saline solution, then diluted in 40 mL of saline. Upon

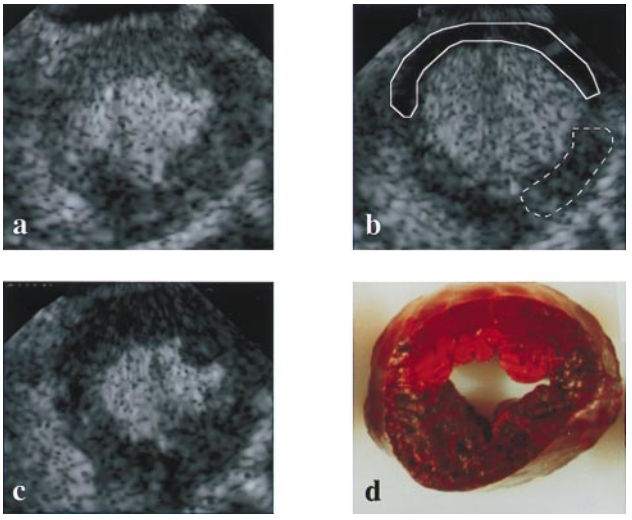

Figure 1. Example is shown of a MCE study and the corresponding anatomic myocardial slice. **a,** The LV short axis recorded at baseline during the infusion of AF0150 and ECG-gated harmonic imaging. **b,** During coronary occlusion, the LAD risk area was delineated by MCE as an area of absent videointensity (**solid outline**) and, **d,** corresponded to the anatomic risk area defined by the unstained area at Monastral blue dye. **b,** The control area in the circumflex perfusion territory is outlined in dots. **c,** After 3 h of reperfusion, the videointensity within the risk area decreased relative to its baseline value.

reconstitution, the agent yields a dispersion of surfactant-coated, perfluorohexane/nitrogen-containing microbubbles. The median diameter of these microbubbles is approximately 5 μm. Myocardial enhancement was achieved by a continuous infusion of 4 mg/min, and images were obtained during infusion after myocardial videointensity had reached a plateau.

Data were recorded on S-VHS videotape with a high-fidelity video recorder and also acquired in a digital format on-line using the Integrated Stress Echo Module (Nova Microsonics). The digital short axis views were analyzed using the NIH Image 1.62 software package to delineate the endocardial and epicardial borders, excluding the bright edge reflectors. Custom-designed software (V.B. and K.O.) was then used to obtain videointensity measurements from the myocardium (0–255 gray levels). The risk area was identified as the transmural area of absent contrast enhancement observed after injection of contrast during coronary occlusion. At each protocol data point, background-subtracted videointensity was calculated for the risk area and for an adjacent control myocardial zone in the perfusion territory of the circumflex (LCx). Care was taken to limit the control zone so as to exclude areas of signal attenuation and/or artifacts (Fig. 1). Videointensity measurements were expressed as the ratio of the average intensity in the risk area to the average intensity in the control zone. In this way, we eliminated the effects of attenuation and other technical factors, as well as variations from injection to injection and from animal to animal, which could have influenced the results. At each data collection point, percent regional myocardial thickening was calculated from the center of the risk area using the formula: [(systolic

Table 1. Hemodynamic Data

	Baseline	Occlusion	Rep 5 min	Rep 30 min	Rep 90 min	Rep 3 h
Heart rate (beats/min)	124.2 ± 3.7	120.1 ± 4.38	112. ± 6.3	104.7 ± 3.8*	99.7 ± 4*	100.8 ± 4.4*
Mean Pulm P (mm Hg)	16.5 ± 0.7	19 ± 1*	21.1 ± 1*	20.4 ± 0.9*	20 ± 1.2*	20.2 ± 1*
Wedge P (mm Hg)	6.3 ± 0.7	7.37 ± 0.8	8 ± 0.8	7.7 ± 0.5	7.2 ± 0.4	7.3 ± 0.4
Mean Art P (mm Hg)	106.2 ± 4.8	96.4 ± 5	80.2 ± 3.8*	76 ± 3.2*	65.1 ± 3.7*	63.8 ± 4.5*
LV P (mm Hg)	115.2 ± 5.1	101.4 ± 5.5†	87.4 ± 4.9*	84.8 ± 3.2*	76.6 ± 3.2*	84 ± 4.3*
LVedp (mm Hg)	4.7 ± 0.6	6.5 ± 1	6.7 ± 0.9	7.3 ± 0.9	7.9 ± 1.3*	7.5 ± 1.4†
CO (l/min)	3 ± 0.2	2.2 ± 0.1*	2.1 ± 0.2*	1.9 ± 0.1*	1.79 ± 0.1*	1.8 ± 0.1*
Thickening (%)	100	17.6 ± 17.6*	9.7 ± 10.3*	−1.0 ± 8.4*	0.4 ± 7.4*	3 ± 10.8*

*$p < 0.005$ vs. baseline; †$p < 0.05$ vs. baseline. Art = arterial; CO = cardiac output; edp = end-diastolic pressure; P = pressure; Pulm = pulmonary; Rep = reperfusion.

thickness − diastolic thickness)/diastolic thickness]·100, and expressed as the percentage of the baseline value.

Myocardial blood flow measurement. Myocardial blood flow was measured by standard techniques (20). Briefly, approximately, 3×10^6 15-μm fluorescent microspheres (Nuflow Spheres; Triton Technology Inc.) were injected directly into the left atrium. Reference blood samples were simultaneously withdrawn from the femoral artery with a constant rate pump (Harvard '33' syringe pump) at a withdrawal rate of 15 mL/min. After the animal was euthanized, the heart was explanted and sliced, and the cross-sectional slice of the LV corresponding to the echo short-axis image was cut into 12 wedge-shaped transmural tissue samples for blood flow analysis. The tissue and the arterial reference samples were processed using a flow cytometer to count the microspheres. The value of RBF was derived for the risk area and for the control zone, and their ratio (risk area/control) was calculated.

Determination of perfusion defect, risk area, and infarct size. After the completion of the experimental protocol, the risk area was delineated by reoccluding the LAD and injecting a 1 mg/kg bolus of Monastral blue dye into the left atrium. The dog was euthanized and the heart was explanted. The right ventricle and the atria were removed and the left ventricle cut into six slices parallel to the atrioventricular groove. The myocardial slice corresponding to the echo short axis image was incubated in a 2% solution of 2,3,5-triphenyltetrazolium chloride (TTC) for 20 min at 37°C, and the infarct was identified as the region that failed to demonstrate brisk red staining. The LV slice was then photographed in color and the outlines of the entire slice, the risk area, and the infarct size were traced on transparencies and their area calculated by digital planimetry (NIH Image 1.62).

Experimental protocol. For each animal, hemodynamics, RBF and MCE data were acquired at baseline, at the end of the occlusion period, and during four time points during reperfusion (5, 30, 90, and 180 min). After the collection of the last data point, the heart was sliced and processed for measurements of risk area, infarct size, and RBF.

Statistical methods. Data from all animals were expressed as mean ± SEM. Correlation between MCE and RBF data was performed by linear regression analysis. Comparisons of hemodynamics, RBF, and MCE data were performed using repeated-measures ANOVA, and Bonferroni *t* test was used to assess the statistical difference between multiple comparisons. A value of $p < 0.05$ (two-sided) was considered statistically significant.

Results

All 16 animals completed the study protocol and technically adequate images were obtained from each experiment. Hemodynamic data for the entire study group are presented in Table 1. The hemodynamic changes observed were attributed to the open-chest model of prolonged coronary occlusion and reperfusion (21). During coronary occlusion, regional myocardial thickening of the risk area was significantly reduced to 20% of the baseline value. During reperfusion, regional myocardial thickening progressively decreased until it was nearly absent after 30 min of reflow (Table 1).

The risk area of the study population was 43 ± 4% of the left ventricle, and the infarct size was 28 ± 4% of the risk area. Figure 1d shows an example of the definition of risk area by blue dye and infarct size by TTC staining.

Temporal changes of regional myocardial blood flow. Myocardial blood flow exhibited dynamic changes during this protocol (Fig. 2). At baseline, RBF within the risk area was comparable with that of the control zone (risk area/control ratio = 0.92 ± 0.02). During coronary occlusion, RBF ratio was significantly reduced from baseline ($p < 0.0001$). Five minutes after coronary artery reopening, a significant hyperemic response was observed within the risk area with consequent increase in RBF ratio ($p < 0.0001$ vs. baseline). After 30 min of reperfusion, RBF ratio returned to baseline values. Blood flow within the risk area was then progressively reduced over time and RBF ratio reached a value lower than baseline at 90 min of reflow ($p < 0.0001$ vs. baseline) with further reduction at 180 min of reperfusion (Fig. 2). Thus, RBF ratio was characterized by a decrease with occlusion, an increase immediately after reperfusion, and a subsequent fall after 90 min of reflow with further reduction at 180 min to levels below those of baseline.

Myocardial contrast echocardiography. Videointensity values also varied during the protocol in a pattern identical to that of RBF (Fig. 2). At baseline, similar videointensity in the

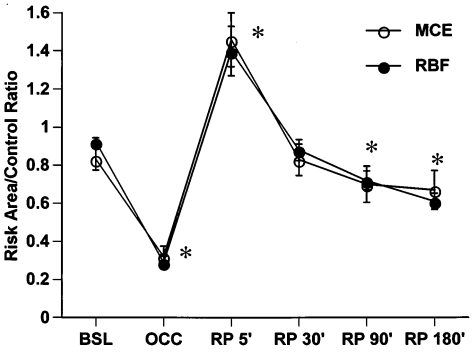

Figure 2. This graph displays the changes over time of risk area/control area ratios of videointensity obtained from MCE and RBF in this study. Values are reported at baseline **(BSL),** during LAD occlusion **(OCC),** and at 5, 30, 90, and 180 min of reperfusion **(RP).** Both MCE and RBF ratios follow the same trend and their values are identical at each time point. Both parameters decreased significantly during coronary occlusion and increased over baseline at 5 min of reperfusion (*$p < 0.0001$ vs. baseline). At 30 min of reperfusion, both MCE and RBF ratios returned to baseline values and then progressively decreased at 90 and 180 min of reperfusion to a level lower than baseline (*$p < 0.0001$ vs. baseline for RBF).

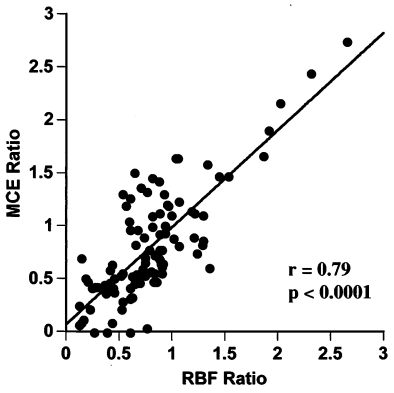

Figure 4. Linear correlation between MCE ratio and RBF ratio for all the data points in this study.

risk area and control zone support our visual observation of uniform myocardial opacification of the LV short axis (Fig. 1a). During coronary occlusion, a minimal contrast effect detected in the risk area was interpreted as noise or as reflecting the presence of intramyocardial collateral flow. The videointensity ratio increased above baseline 5 min after reopening the vessel, then returned to baseline in the first 30 min of reperfusion and subsequently manifested a small progressive decline throughout reperfusion in a fashion similar to that seen with RBF (Fig. 2). Figure 3 shows a series of ultrasound images acquired during a representative MCE study.

At each time point during occlusion and reperfusion, measurements of videointensity ratio showed a good correlation with those of flow (MCE = 0.07 + 0.91 × RBF; r = 0.79; $p < 0.0001$), as shown in Figure 4.

Discussion

This study delineated a pattern of microvascular perfusion during postischemic reflow characterized by an immediate hyperemic response followed by a prompt return toward baseline and then a progressive reduction of flow. MCE performed with intravenous AF0150 and ECG-gated harmonic imaging consistently delineated this pattern and yielded values for reperfusion flow that correlated closely with those determined by microspheres. Thus, these data provide the basis for an important role for MCE in the assessment of reperfusion microcirculatory flow.

Time course of postischemic microvascular perfusion. Regional microvascular perfusion after coronary reflow reflects the status of the microvasculature. A prolonged, but reversible, ischemic injury produces functional and structural abnormalities of both the myocardium and the microvasculature. If the patency of the epicardial vessel is restored after 90 min of ischemia, blood flow within the myocardium may be partially or totally absent in areas of damaged and obstructed microvasculature (6). Such no- or low-reflow areas have been demonstrated to show little improvement of regional and global myocardial function at follow-up and a higher incidence

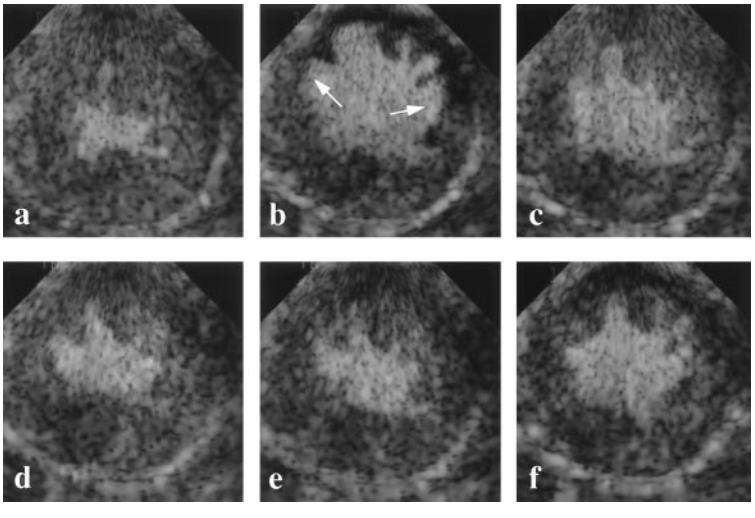

Figure 3. This figure shows a representative MCE case demonstrating the progressive changes in videointensity observed within the risk area during coronary occlusion and reperfusion. **a,** The contrast-enhanced LV short axis at baseline. The infusion of the contrast agent and the ECG-gated harmonic imaging yielded uniform myocardial opacification with no attenuation of the posterior wall. **b,** The risk area is delineated by absent contrast enhancement during LAD occlusion (between **arrows**). **c,** Five min after the release of the coronary occlusion, an increase in videointensity is noted within the postischemic myocardium, which correlated with the hyperemic flow detected by microspheres. **d, e,** and **f,** The MCE images acquired at 30, 90, and 180 min of reperfusion, respectively. A clear progressive reduction in videointensity can be observed within the risk area.

of adverse clinical events (11,12,22). Furthermore, even though reestablishing flow after prolonged ischemia can reduce the infarct size, it might also be responsible for additional myocardial and microvascular damage to that induced by the ischemia (5–7).

Reperfusion is a dynamic phenomenon, characterized by serial changes in flow in the postischemic microcirculation. The precise time-course of changes in reflow remains controversial. A study by Ambrosio et al. (6) reported the time-course of postischemic reflow in a canine model of 90 min of reversible coronary occlusion. After an initial hyperemic phase (2 min after reflow), RBF was progressively reduced over the 210-min period of observation. However, another report (23), which studied 3 h of reversible coronary occlusion in canines, could not demonstrate a clear trend toward flow reduction within the risk area over 3 h of reperfusion. The reason for this discrepancy is uncertain; it has been suggested to be related to the different duration of occlusion. However, data in our study demonstrated that after 180 min of coronary occlusion, myocardial blood flow and videointensity had a trend in progressive reduction during reperfusion similar to that observed after 90 min of occlusion. Moreover, after the longer coronary occlusion, we observed lower flow and videointensity values throughout reperfusion. Thus, the current data support the existence of a progressive reduction of microvascular reperfusion after transient coronary occlusion.

Myocardial contrast echo in the evaluation of postischemic reperfusion. MCE has unique potential for the in vivo assessment of the amount and spatial distribution of microvascular patency, myocardial blood flow, and volume (17,24–26). If properly engineered, gas microbubbles injected into the blood stream can flow freely within the microvasculature with a rheologic behavior similar to that of red blood cells (27). Ultrasound can detect passage of these microbubbles within the microcirculation and display an image with information on the location and concentration of bubbles within the myocardium that reflects the topographic distribution and density of patent coronary microvessels (24).

In humans, all the currently available information regarding postischemic reperfusion derives from MCE studies in which microbubble agents have been injected directly into the coronary circulation (11–15). Recent improvements in engineering of the bubbles have resulted in a new generation of contrast agents suitable for the study of myocardial perfusion during intravenous administration (18,19). Early experimental studies in animals have demonstrated that MCE obtained with intravenous infusion of perfluorocarbon-based contrast agents can accurately define myocardial area at risk during coronary occlusion and infarct size during reperfusion (28). The current data expand these potential applications to include the determination of postocclusion microcirculatory flow.

In this study, we elected to use harmonic imaging as opposed to fundamental imaging. The superior efficacy of harmonic methods in bubble detection and quantitation over fundamental mode has been demonstrated (29,30). In addition, to avoid attenuation of far field signals and saturation of the instrument due to high concentration of bubbles, only a small dose of the contrast agent was administered in the form of a continuous infusion. The detection of the small number of resonant bubbles injected was amplified by delivering the ultrasound energy gated to the ECG in order to limit their dissolution (31).

Limitations of the study. In this study we used the videointensity of the contrast effect within the myocardium as an estimate of myocardial blood flow. Although it has been shown that peak myocardial videointensity is primarily related to myocardial blood volume (32), changes in myocardial blood volume can be reflected via changes in flow. We observed a close relationship between myocardial videointensity and RBF, suggesting that the changes in flow observed were coupled with alterations of blood volume. Moreover, it is known that videointensity loses its linear relationship with flow at high flow values (32). Therefore, we were careful to adjust the instrument settings and select the contrast dose in order to remain within the linear range of videointensity and flow during the entire experiment. Also we measured the ratio of videointensity between two beds (LAD and LCx), which obviated the need for a strict linear relation between microbubble concentration and flow, since the relative changes in bubble concentration were compared with the corresponding changes in microsphere blood flow.

Only one triggering interval (once every six beats) was used in this study, and was selected since it appeared to achieve optimal, uniform myocardial opacification at the dose of contrast and machine settings used. Other intervals, especially in conjunction with other agents, may yield different results. Also, we used only a single contrast agent in this study, whose advantages and limitations compared with other agents cannot be defined by our protocol.

We did not attempt to unmask any possible abnormalities of the vasodilatory reserve of the coronary microcirculation. It is well known that impairment of this reserve is the earliest change induced by the ischemic injury (9,33), and MCE has been demonstrated to reliably detect this abnormality (23). Therefore, it is conceivable that if a vasodilator had been used in this study, myocardial blood flow and contrast videointensity would have been further impaired at each stage of reperfusion relative to the control area. However, examination of microvascular flow reserve was not one of the aims of this study. In addition, the value of assessing flow reserve in the clinical practice remains to be determined. Additional studies specifically designed to address this issue are needed.

The coronary occlusion produced in this study was completely and instantaneously reversed. A longer delay before reperfusion or persistence of a residual stenosis, such as often occurs with thrombolysis in the clinical arena, may theoretically change the time-course and the amount of myocardial reflow. The presence of multivessel disease might also influence the results obtained. The role of these variables remains to be investigated.

Clinical implications. The results of this experimental study have potential clinical implications. Reopening of the

infarct-related vessel is currently attempted in the majority of patients with acute myocardial infarction in order to reestablish flow to the myocardium and limit infarct size. However, the efficacy of recanalization therapy in achieving reperfusion at the level of postischemic myocardium cannot be assumed from the successful reopening of the epicardial vessel. Absence of microvasculature integrity after acute myocardial infarction implicates more extensive necrosis and greater functional impairment, as shown by more pronounced cardiac enzyme elevation and more severe regional contractility deterioration (11–15). Because of the functional importance of the microvasculature during ischemia-reperfusion, the variable severity of impairment during reperfusion, and because of the recently demonstrated ability of calcium antagonists to limit microvascular dysfunction after acute infarction (16), serial evaluation of both the extent and severity of microvascular impairment is of great clinical importance both in the acute and subacute phase of infarction. Our data establish that MCE has the potential to yield such information.

We are particularly grateful to Barry Peters, MD, Jim Reynolds, and Jessica Weigenseil for their valuable technical support during the study protocol, and to Jeff Powers, PhD of ATL for his assistance in optimizing the settings for the echocardiographic system.

References

1. Krug A, Du Mesnil de Rochemont, Korb G. Blood supply of the myocardium after temporary coronary occlusion. Circ Res 1966;19:57–62.
2. Kloner RA, Ganote CE, Jennings RB. The "no reflow" phenomenon after temporary coronary occlusion in the dog. J Clin Invest 1974;54:1496–508.
3. White FC, Sanders M, Bloor CM. Regional distribution of myocardial blood flow after coronary occlusion and reperfusion in the conscious dog. Am J Cardiol 1978;42:234–43.
4. Kloner RA, Ellis SG, Lange R, Braunwald E. Studies of experimental coronary artery reperfusion: effects on infarct size, myocardial function, biochemistry, ultrastructure and microvascular damage. Circulation 1983; 68(Suppl I):8–15.
5. Engler RL, Schmid-Schönbein GW, Pavalec RS. Leukocyte capillary plugging in myocardial ischemia-reperfusion in dog. Am J Phatol 1983;111:98–111.
6. Ambrosio G, Weisman HF, Mannisi JA, Becker LC. Progressive impairment of regional myocardial perfusion after initial restoration of postischemic blood flow. Circulation 1989;80:1846–61.
7. Jeremy RW, Links JM, Becker LC. Progressive failure of coronary flow during reperfusion of myocardial infarction: documentation of the no reflow phenomenon with positron emission tomography. J Am Coll Cardiol 1990; 16:695–704.
8. Cobb FR, Bache RJ, Rivas F, Greenfield JC. Local effects of acute cellular injury on regional myocardial blood flow. J Clin Invest 1976;57:1359–68.
9. Tsao PS, Aoki N, Lefer DJ, Johnson G, Lefer AM. Time course of endothelial dysfunction and myocardial injury during myocardial ischemia and reperfusion in the cat. Circulation 1990;82:1402–12.
10. Forman MB, Puett DW, Virmani R. Endothelial and myocardial injury during ischemia-reperfusion: pathogenesis and therapeutic implications. J Am Coll Cardiol 1989;13:450–9.
11. Ito H, Tomooka T, Sakai N, et al. Lack of myocardial perfusion immediately after successful thrombolysis. A predictor of poor recovery of left ventricular function in anterior myocardial infarction. Circulation 1992;85:1699–705.
12. Ito H, Iwakura K, Oh H, et al. Temporal changes in myocardial perfusion patterns in patients with reperfused anterior wall myocardial infarction. Their relation to myocardial viability. Circulation 1995;91:656–62.
13. Lim Y, Nanto S, Masuyama T, Kohama A, Hori M, Kamada T. Myocardial salvage: its assessment and prediction by the analysis of serial myocardial contrast echocardiograms in patients with acute myocardial infarction. Am Heart J 1994;128:649–56.
14. Iliceto S, Galiuto L, Marchese A, et al. Microvascular integrity, contractile reserve and myocardial viability after acute myocardial infarction. Am J Cardiol 1996;77:441–5.
15. Iliceto S, Galiuto L, Marchese A, Colonna P, Oliva S, Rizzon P. Functional role of microvascular integrity in patients with infarct related artery patency after acute myocardial infarction. Eur Heart J 1997;18:618–24.
16. Taniyama Y, Ito H, Iwakura K, et al. Beneficial effect of intracoronary verapamil on microvascular and myocardial salvage in patients with acute myocardial infarction. J Am Coll Cardiol 1997;30:1193–9.
17. Kaul S, Kelly P, Oliner JD, et al. Assessment of regional myocardial blood flow with myocardial contrast two-dimensional echocardiography. J Am Coll Cardiol 1989;13:468–82.
18. Porter TR, Xie F, Kricsfeld A, Kilzer K. Noninvasive identification of acute myocardial ischemia and reperfusion with contrast ultrasound using intravenous perfluoropropane-exposed sonicated dextrose albumine. J Am Coll Cardiol 1995;26:33–40.
19. Mulvagh SL, Foley DA, Aeschbacher BC, Klarich KK, Seward JB. Second harmonic imaging of an intravenously administered echocardiographic contrast agent: Visualization of coronary arteries and measurement of coronary blood flow. J Am Coll Cardiol 1996;27:1519–25.
20. Austin GE, Martino-Salzman D, Justicz AG, et al. Determination of regional myocardial blood flow using fluorescent microspheres. Am J Cardiovasc Path 1993;4:352–7.
21. Reimer KA, Jennings RB, Cobb FR, et al. Animal models for protecting ischemic myocardium: results of the NHLBI Cooperative Study. Comparison of unconscious and conscious dog models. Circ Res 1985;56:651–65.
22. Ito H, Maruyama A, Iwakura K, et al. Clinical implications of the "no reflow" phenomenon. A predictor of complications and left ventricular remodeling in reperfused anterior wall myocardial infarction. Circulation 1996;93:223–8.
23. Villanueva FS, Glasheen WP, Sklenar J, Kaul S. Characterization of spatial patterns of flow within the reperfused myocardium by myocardial contrast echocardiography. Circulation 1993;88:2596–2606.
24. Kaul S, Glasheen W, Ruddy RD, et al. The importance of defining left ventricular area at risk in vivo during acute myocardial infarction: an experimental evaluation with myocardial contrast echocardiography. Circulation 1987;75:1249–60.
25. Mor-Avi V, Lang RM, Robinson KA, et al. Contrast Echocardiographic quantification of regional myocardial perfusion: validation with an isolated rabbit heart model. J Am Soc Echocardiography 1996;9:156–65.
26. Lindner JR, Skyba DM, Goodman NC, Jayaweera AR, Kaul S. Changes in myocardial blood volume with graded coronary stenosis: an experimental evaluation using myocardial contrast echocardiography. Am J Physiol 1997; 272:H567–75.
27. Jayaweera AR, Edwards N, Glasheen WP, et al. In vivo myocardial kinetics of air-filled albumin microbubbles during myocardial contrast echocardiography: comparison with radiolabeled red blood cells. Circ Res 1994;74:1157–65.
28. Grayburn PA, Erickson JM, Escobar J, Womack L, Velasco CE. Peripheral intravenous myocardial contrast echocardiography using a 2% dodecafluoropentane emulsion: identification of myocardial risk area and infarct size in the canine model of ischemia. J Am Coll Cardiol 1995;26:1340–7.
29. Burns PN, Powers JE, Simpson DH, Uhlendorf V, Fritzsche T. Harmonic imaging: principles and preliminary results. Clin Radiol. 1996;51(Suppl I):50–5.
30. Firschke C, Lindner JR, Goodman NC, Skyba DM, Wei K, Kaul S. Myocardial contrast echocardiography in acute myocardial infarction using aortic root injections of microbubbles: potential application in the cardiac catheterization laboratory. J Am Coll Cardiol 1997;29:207–16.
31. Porter TR, Xie F. Transient myocardial contrast after initial exposure to diagnostic ultrasound pressures with minute doses of intravenously injected microbubbles: demonstration and potential mechanisms. Circulation 1995; 92:2391–5.
32. Wiencek JG, Feinstein SB, Walker R, Aronson S. Pitfalls of quantitative contrast echocardiography: the steps to quantitation of perfusion. J Am Soc Echocardiography 1993;6:395–416.
33. Vanhaecke J, Flameng W, Borgers M, Jang IK, Van de Werf F, De Geest H. Evidence for decreased coronary flow reserve in viable postischemic myocardium. Circ Res 1990;67:1201–10.